Molecular-dynamics investigation of hydrogen hopping in palladium

J. W. Culvahouse
Department of Physics and Astronomy, University of Kansas, Lawrence, Kansas 66044

Peter M. Richards
Sandia National Laboratories (Division 1112), Albuquerque, New Mexico 87185-5800
(Received 22 January 1988; revised manuscript received 27 June 1988)

Diffusive hopping of hydrogen in PdH_x has been reexamined with molecular-dynamics (MD) simulations in order to clarify earlier results of Gillan. We obtain the same values for the diffusion coefficient and width Γ_q of the quasielastic neutron scattering function when Gillan's potentials are used, but go beyond Gillan in performing a statistical analysis of the jumps. The analysis shows that over 95% of the jumps are uncorrelated and nearest neighbor, but the distribution of times between jumps is highly nonexponential. This latter feature accounts for the departure of Γ_q, noted by Gillan, from the Chudley-Elliott (CE) theory based on simple one-step nearest-neighbor hopping. A simple physical model of the hopping as a two-step process can explain the results and suggests they are highly sensitive to the H-Pd potential at short distances. A new MD simulation with a harder-core potential gives a Γ_q in much better agreement with CE. We conclude that the non-CE behavior originally found by Gillan might be seen in real experiments on systems with suitably soft potentials.

I. INTRODUCTION

Molecular dynamics (MD) has proved a powerful tool for studying both equilibrium and dynamical properties of condensed-matter systems.[1] Of particular interest here has been the usefulness of MD in modeling diffusion of vacancies and interstitials in crystalline solids. Because MD uses classical equations of motions, its relevance can be questioned for the motion of light atoms such as hydrogen which show quantum effects. Nonetheless Gillan[2] has obtained interesting results for hydrogen diffusion in palladium at temperatures sufficiently high (up to 967 K) that classical over-barrier hopping should dominate quantum tunneling. Although Gillan obtained a diffusion coefficient D in agreement with experiment, the simulation results did not agree with quasielastic neutron scattering (QNS) data[3] for large momentum transfer. Gillan attributed this disagreement to aspects of the particle motion in the simulations which he variously described as correlated jumps and multiple jumps. He pointed to improper potentials, neglect of quantum effects, and neglect of interactions with conduction electrons as possible reasons for the failure of the simulations to account for the experimental results. On the basis of fragmentary work using other potentials, he was inclined to doubt that the potential was a major source of the discrepancy. In this paper we find that the results are in fact strongly influenced by the Pd-H potential. We show, that with a suitably soft potential as used by Gillan, it is perfectly reasonable on physical grounds to obtain the hopping behavior found by Gillan and described below. Although this behavior apparently has not been seen[3,4] in PdH_x it may occur in other systems.[5] Our own MD calculations give the same "raw data" as Gillan, but we give a different interpretation of the hydrogen jumps that is based on statistical analysis and careful definition of what is meant by a "jump" when dealing with continuous MD trajectories.

The behavior found by Gillan and us is directly related to the width Γ_q of the dynamical structure factor $S(\mathbf{q},\omega)$ observed in QNS.[3] For a single particle undergoing a random walk with nearest-neighbor jumps, Γ_q is given by the well-known Chudley-Elliott (CE) expression[6]

$$\Gamma_q = \Omega(1-\gamma_q) , \tag{1}$$

where $\gamma_q = (1/Z)\sum e^{i\mathbf{q}\cdot\boldsymbol{\delta}_i}$ with the sum going over the Z values of nearest-neighbor displacements $\boldsymbol{\delta}_i$ of magnitude $\delta_i = \delta$ and where, for a cubic lattice, the characteristic jump rate is related to the diffusion coefficient by $\Omega = 6D/\delta^2$. As illustrated in Fig. 1, the MD simulation shows Γ_q to have a weaker dependence on q than given by the CE expression (1). It instead has a form closely resembling Eq. (9) below. Since neutron data for PdH_x seem to be in accord with CE, Gillan suspected there may be a fundamental problem with the simulation. From an examination of the trajectories, Gillan concluded that there were nearest-neighbor jumps, but they were strongly correlated in that particles which had jumped tended to jump again very quickly with a persistence of direction, and that this was a likely source of the discrepancy. He noted that such persistence of jumps could result from an insufficient rate of energy transfer between hydrogen and the lattice. If this were due to effects other than the choice of potentials, it obviously would have serious implications for the use of MD in studying the dynamics.

Section II describes our own simulation and analysis of the distribution of jump times. This analysis is not trivial because some care has to be used in translating MD tra-

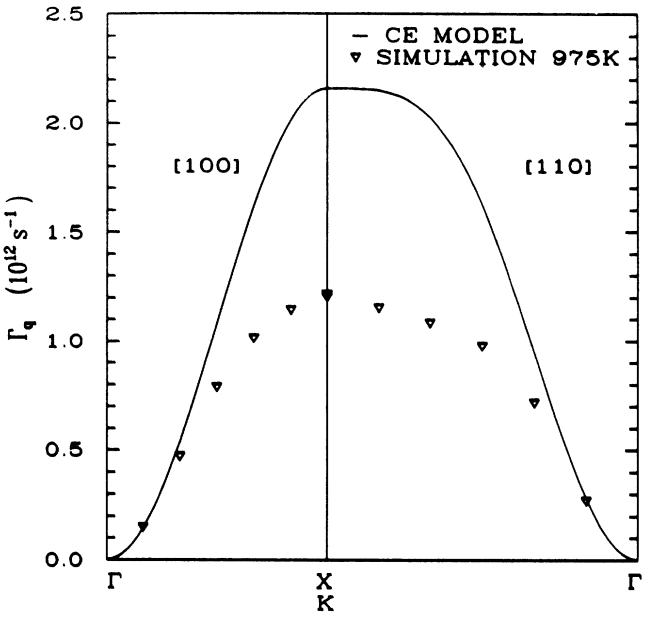

FIG. 1. Comparison of Γ_q from simulations using Gillan's potentials with the CE model for points in the first Brillouin zone along the [100] and [110] directions. The constant Ω in Eq. (1) is chosen to fit the data at small q.

jectories into what can reasonably be classified as jumps. Although, for the same potentials used by Gillan, we find the same behavior of Γ_q, the analysis shows that the vast majority of jumps are essentially uncorrelated hops to nearest-neighbor sites but there is a highly nonexponential distribution of residence times which leads to the departure from CE. We then show MD results using a metal-hydrogen potential with a stronger repulsion at short distances. This new potential gives a more nearly exponential jump-time distribution and Γ_q in closer agreement with CE (1). We therefore conclude that the difference between Gillan's results and CE and the QNS data for PdH_x were caused largely by choice of potential.

In Sec. III we present a simple two-level model for the jumping process which illustrates how strong departures from Eq. (1) can result even if the hopping is uncorrelated and restricted to nearest neighbors. The deviation from Eq. (1) or CE depends on the ratio between the rate W to jump between sites from levels at the top of a potential well and the rate w to equilibrate between these levels and ones at the bottom of the well. CE requires $W \ll w$, i.e., rapid equilibration at a site before a jump occurs, whereas the MD data for the relatively soft potential are consistent with $W \approx w$ so that an appreciable number of jumps occur without a particle being able to come to equilibrium at the site to which it has jumped. This can give the appearance of the particle jumping greater than nearest-neighbor distances (or of correlated NN jumps), since an excited particle can make many nearest-neighbor hops before getting "trapped" in a well. We further argue how giving the potential a more repulsive core can decrease W/w and thus lead to CE behavior, and simulation data are shown in support of this.

Section IV contains a summary and discussion. Included are reasons why we think small-sample-size and quantum effects are not serious problems in our and Gillan's simulations and a discussion of which lattice geometries are likely to be most favorable for having the non-CE behavior.

II. SIMULATION AND ANALYSIS OF JUMP DISTRIBUTION

We reproduced the results of Gillan by following the description given in his paper. We used the same potentials: for the Pd-Pd interactions a power series in r cut off at 3.3 Å which reproduced the experimental phonon dispersion curves of pure Pd at room temperature; for Pd-H a simple exponential $Ae^{-r/\rho}$ cut off at 3.8 Å in which the scale factor ρ was given the value 0.5 Å and A was assigned the value 15.3 eV which reproduces the observed local mode frequency for $PdH_{0.027}$; and the H-H interaction was taken as identical to Pd-H. The lattice constant a was taken as 4.07 Å.

The equations of motion were integrated using the algorithm described by Schofield,[7] and for the reproduction of Gillan's calculations we used a time increment of 2.6125×10^{-15} s, 5% greater than his. The usual periodic boundary conditions were applied. A system of 108 Pd on their fcc sites, and 20 H inserted randomly in the octahedral sites was given a total energy which corresponded to 1025 K using the harmonic approximation for the potential energy. It was found that this produced an average kinetic energy for the system corresponding to 975±2 K, very close to the 967 K used by Gillan for his displayed data. This system was allowed to equilibrate for 4×10^4 steps, and then hydrogen position data were recorded for the next 1×10^5 steps. Since the purpose was to examine the long-time diffusive motion, the hydrogen coordinates were recorded on an absolute basis (i.e., boundary crossings were recorded) and the values recorded were the average over 10 time steps which is about $\frac{1}{3}$ of a vibration period t_H for the hydrogen local mode.

We calculated the diffusion coefficient from the average square displacement of the hydrogen versus time and obtained $D_s=2.27\times10^{-4}$ cm^2/s at 975 K and $D_s=5.69\times10^{-5}$ cm^2/s at 700 K, from which an activation energy of 0.29±0.02 eV was deduced. Our values of D_s and other quantities to be reported agreed with those of Gillan to within better than 5% in all cases where numbers were quoted or could be deduced from figures in Gillan. We also calculated the neutron incoherent scattering function[3]

$$S(\mathbf{q},t)=\langle \exp\{i\mathbf{q}\cdot[\mathbf{r}(t)-\mathbf{r}(0)]\}\rangle \ , \tag{2}$$

in which the triangular brackets denote statistical average.

The Fourier transform of $S(\mathbf{q},t)$ is the dynamical structure factor $S(\mathbf{q},\omega)$, the line-shape function for QNS. The hopping part of $S(\mathbf{q},t)$ is an exponential with damping factor Γ_q, so that $S(\mathbf{q},\omega)$ is Lorentzian with half width at half maximum Γ_q. The effect of vibratory motion is included by introducing a Debye-Waller factor and limiting the validity to times long compared with the

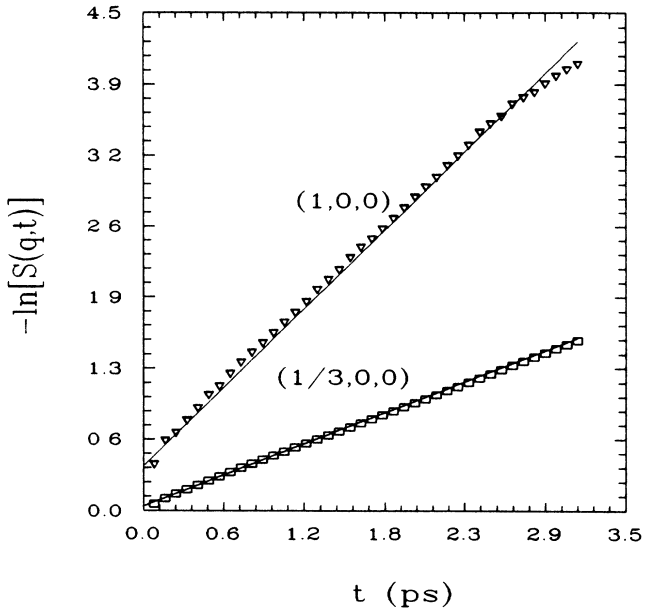

FIG. 2. Semilogarithmic plots of the neutron incoherent scattering function $S(\mathbf{q},t)$ versus time for $\mathbf{q}$ at the edge of the Brillouin zone in the [100] direction and for a point $\frac{1}{3}$ of the way to the edge in the same direction. Also shown are straight lines drawn according to the procedure described in the text used for determining the value of Γ_q for all simulations. Data are for $T=975$ K.

vibrational period, whereby the approximate relation is

$$S(\mathbf{q},t)=e^{-\langle u^2\rangle q^2}e^{-\Gamma_q t}, \tag{3}$$

in which the quantity $\langle u^2\rangle$ in the Debye-Waller factor is related to the mean-square displacement associated with vibrational modes.

Example semilog plots of the $S(\mathbf{q},t)$ from the simulation are shown in Fig. 2 for two values of $\mathbf{q}$, $(2\pi/a,0,0)$ and $(2\pi/3a,0,0)$, where a is the fcc lattice constant. These plots are essentially identical to those of Gillan, except that the data for $(2\pi/a,0,0)$ are smoother than Gillan's as a result of our use of positions averaged over 10 simulation steps. Also shown in the figure are straight lines fit to the data between 1.05 and 2.1 ps, the slope of which is used to determine Γ_q. The simulation results for Γ_q, plotted in Fig. 1, were obtained by this method for a range of $\mathbf{q}$. These agree with Gillan for the $\mathbf{q}$'s which he calculated, but we have calculated twice as many points. [The fact that we have a simulation volume of side $L=3a$ does not limit the validity of $S(\mathbf{q},t)$ to components of $\mathbf{q}$ being multiples of $2\pi/3a$, since we accounted for boundary crossings.] As stated in the Introduction, the simulations disagree drastically with the predictions of the CE model shown as a solid curve in Fig. 1. For this and all other comparisons with CE, the value of Ω in Eq. (1) was chosen to fit the diffusion coefficient. That is, the $q\rightarrow 0$ limit of Γ_q/q^2 was chosen to agree with D obtained from the slope of $\langle r^2\rangle$ versus t.

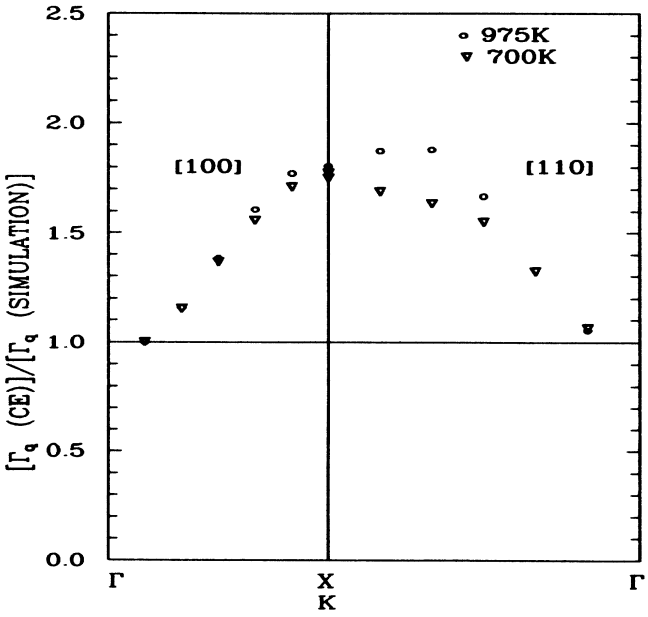

FIG. 3. Comparison of the simulation results at 975 and 700 K to the prediction of CE for points in the first Brillouin zone.

We also calculated the Γ_q's for a simulation at 700 K which is the highest temperature at which experimental data are available. In Fig. 3, we plot the ratio of the simulation Γ_q to the CE prediction for both temperatures. Although the 700 K data show marginally better agreement with CE, there is sizable discrepancy at both temperatures. A much more dramatic temperature dependence might be expected if non-CE behavior were associated solely with "liquidlike" effects setting in at the highest temperature, as has been suggested in regard to superionic conductors.[8]

Gillan speculated that multiple jumps (or correlated NN jumps) might be the reason for this disagreement. Such effects can be approximated in an extension of the CE theory in which fractions α_i of the jumps are to ith nearest neighbors. Considering jumps to the nearest neighbors (NN) and next nearest neighbors (NNN), the QNS linewidth is given by a minor generalization of Eq. (1),

$$\Gamma_q=\Omega[\alpha_1(1-\gamma_q^{(1)})+(1-\alpha_1)(1-\gamma_q^{(2)})] \tag{4}$$

in which $\gamma_q^{(i)}$ is the structure factor for the ith nearest neighbor and α_1 is the fraction of NN jumps. The structure factor for the next nearest neighbor $\gamma_q^{(2)}$ goes to unity at the edge of the first Brillouin zone, and thus can decrease Γ_q from the standard CE prediction.

In Fig. 4, we compare the simulation data with three different models by plotting the ratio of the model predictions to the simulation results. As in Fig. 3, theoretical curves are normalized to give the same Γ_q for $q\rightarrow 0$. For the standard CE model the agreement is totally unsatisfactory as already shown in Fig. 3. For the model just described which includes the possibility of NNN jumps, $(1-\alpha_1)$ was chosen to give a best fit to the value of Γ_q at the edge of the Brillouin zone. The value required corresponds to 30% of all jumps being NNN, but clearly any choice for the fraction of NNN jumps cannot produce a satisfactory fit. This results from the fact that $(1-\gamma_q^{(2)})$ peaks at an intermediate point on paths from the center

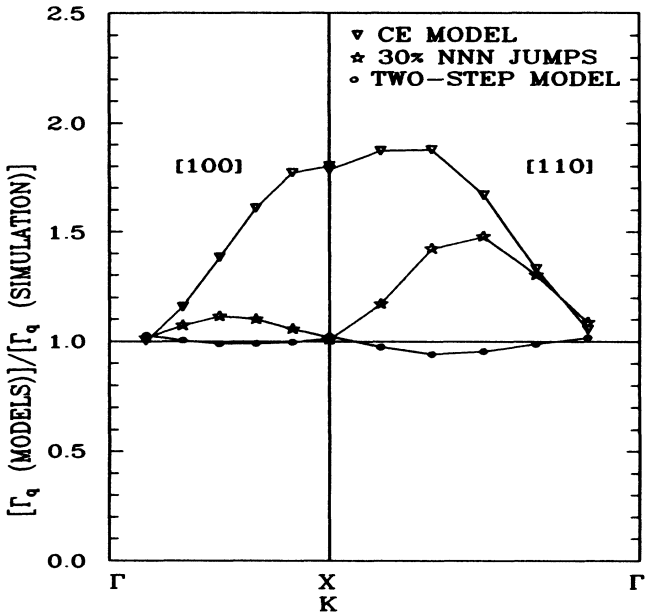

FIG. 4. Comparison of model predictions to the simulation at $T=975$ K for points in the first Brillouin zone. All models have been normalized to give agreement for $q\rightarrow 0$. The points for each model have been connected by lines to aid the eye. The CE model generalized to include 30% NNN jumps produced agreement at the zone edge, but large disagreement remains at intermediate points. The two-step model described in Sec. III yields very good agreement.

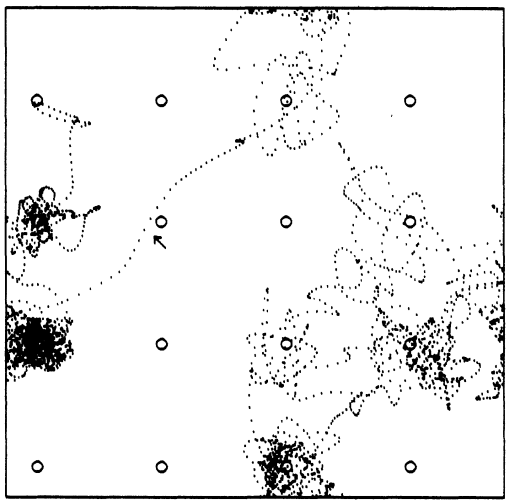

FIG. 5. A projection of the hydrogen motion on a (100) plane for a simulation at 930 K using a simulation volume two unit cells on a side (32 Pd atoms and 6 H atoms). Periodic boundary conditions are imposed at the border of the figure. The open circles identify the projected positions of octahedral sites which lie on alternate planes. The intervening planes contain metal atoms at the same projected positions. The tetrahedral sites project onto points at the center of squares with corners at the open circles and lie in planes between those containing metal ions and octahedral sites. The positions of the H atoms are shown at intervals of $\frac{1}{30}$ of the vibrational period of the hydrogen. A total of 7 ps of the simulation is shown. One part of the path is marked by an arrow and referred to several times in the text.

to the edge of the Brillouin zone. Also displayed in Fig. 4 is the two-level model described in Sec. III, which fits very well.

In Fig. 5 we show examples of single particle trajectories which are very much like those shown by Gillan, who cited them as evidence that multiple jumps are rather frequent. These are projections on a (100) plane. The octahedral sites are identified by open circles. In a single (100) plane only half of the intersections are octahedral sites, the other half being Pd sites. The dots correspond to a single step in the simulation or about $\frac{1}{30}$ of a vibration period for the hydrogen. The simulation volume used for this example is two unit cells on a side and periodic boundary conditions have been imposed so that paths exiting one side of the square will reenter at the other side.

Plots of this type show clearly that the hydrogen spend most of their time at octahedral sites. The time sequence is not transparent in such displays, but from viewing many of these one does note that once a particle jumps, it tends to jump again very shortly afterward, and one can occasionally spot elements of the trajectories which appear to go almost directly between two sites that are not nearest neighbors. Such an example is identified in Fig. 5 by an arrow. Examination of this trajectory step-by-step in three dimensions shows that the particle passed very close to the intermediate octahedral site, but hardly paused there.

The nature of the trajectories is better appreciated by plotting the x,y,z coordinates for selected H atoms as a function of time as in Fig. 6(a). The time interval, sample volume, and boundary conditions are the same as in Fig. 5. The horizontal lines are the coordinates for the octahedral sites. A jump between NN octahedral sites requires that the center of oscillation for two of the three coordinates change from one of the lines to an adjacent one. This example shows four jumps which are indicated by the arrows in the figure. The transitions occur in the order of 10 to 30 time steps. In Fig. 6(b) we plot the coordinates averaged over 10 time steps and for a period six times as long. The longer time view and suppression of the rapid vibration make well-separated jumps easy to pick out, but for closely spaced jumps a very careful analysis is required. The example shown exhibits burst of jumps which is a characteristic reported by Gillan. However this qualitative observation is not necessarily evidence of correlated or non-NN jumps which would explain non-CE behavior. Even the CE model could give the impression of this effect simply because short residence times are more probable than long ones for an exponential distribution of residence times, as expected with normal random hopping. A quantitative study of the distribution of residence times is required. This also requires a precise definition of what is meant by "residence time" and identification of when a jump occurs. Such quantities would be evident in a Monte Carlo simulation where discrete hopping is built into the picture, but they are much less transparent in MD which

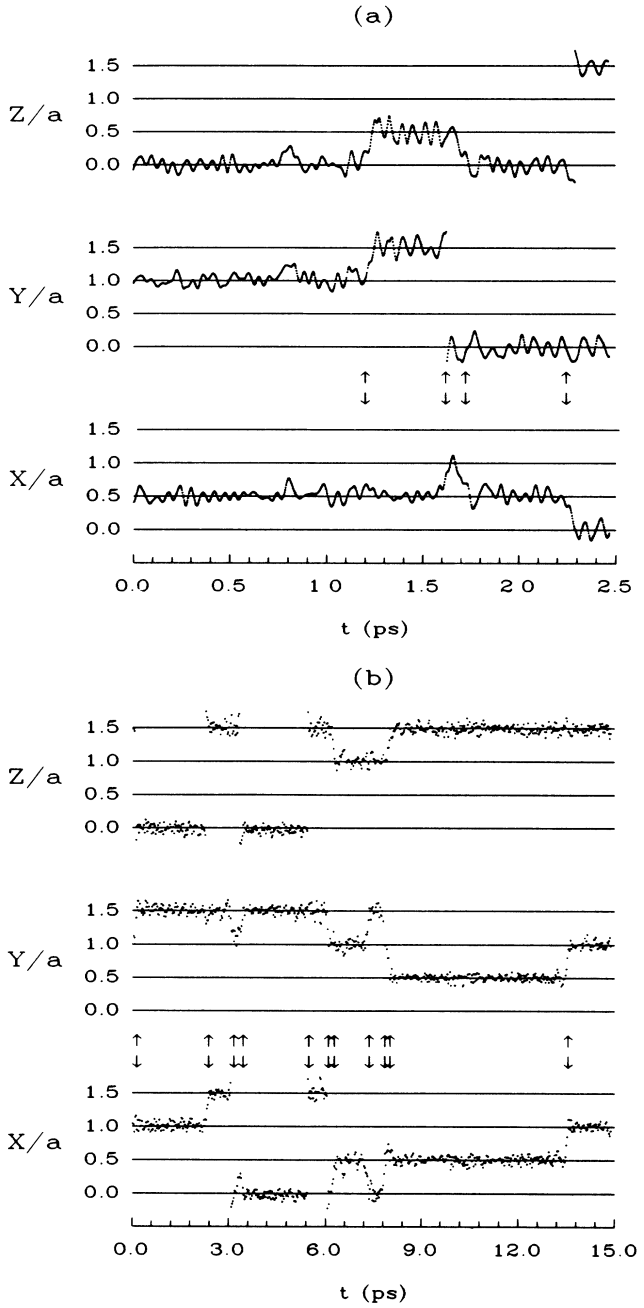

FIG. 6. (a) A plot of the coordinates of a typical hydrogen atom during a simulation using a simulation volume two unit cells on a side. The horizontal lines represent the coordinates of octahedral sites. A transition from one octahedral site to a neighboring one requires that two of the three coordinates change from one line to a neighboring line. (Because of periodic boundary conditions the top and bottom lines are neighbors.) The points are spaced at $\frac{1}{30}$ of a hydrogen vibration period. The double arrows between the X and Y plots identify NN jumps. Note the excursion at 0.8 ps which satisfies the criteria for an excursion to a tetrahedral site. (b) A similar plot but using positions averaged over $\frac{1}{3}$ of a hydrogen vibration period, and over a longer time period. Visual determination of many of the jumps is very tedious. The arrows as in (a) indicate the times at which the computer algorithm called jumps. This sample contains no true NNN jumps, but in several instances the NN jumps are barely resolved.

deals with continuous paths and finite velocities.

The statistical study of the jumps was done by automating criteria suggested by the data in Fig. 6(b). This procedure is designed to give the best description of the motion possible in terms of jumps between NN and NNN octahedral sites. Most of the time as shown clearly in Fig. 6(a), these are well-defined NN jumps. These occur by trajectories that are near to the path $0 \rightarrow S_t \rightarrow T \rightarrow S_t' \rightarrow 0'$ shown in Fig. 7. In a few cases the H gets to a NNN site without passing particularly close to a NN site. These appear to be cases in which the trajectory is near to the path $0 \rightarrow S_t \rightarrow T \rightarrow S \rightarrow T' \rightarrow S_t'' \rightarrow 0''$. That the rate for these NNN jumps is much less than for NN jumps is supported by Gillan's observation that the average density of H at the S point is nearly an order of magnitude smaller than at any point along the diagonal path $0 \rightarrow S_t \rightarrow T$.

We analyzed the jumps using the hydrogen coordinates averaged over 10 time steps as in Fig. 6(b). The first positions were used to assign the H atoms to octahedral sites. If the reduced coordinates fell within a cube of side $a/2$ centered at an octahedral site, they were assigned to that octahedral site. If these initial positions were not in such cubes (which means they are in cubes of the same size centered on the Pd sites) the hydrogen atom was assigned to the nearest octahedral cube. Subsequently, the position of the hydrogen relative to its assigned site was monitored at intervals of 10 time steps. These coordinates were rounded to integer multiples of $a/2$, and the changes in the rounded coordinates relative to the last assigned octahedral site were examined. When these changed in a way which indicated a jump to a new octa-

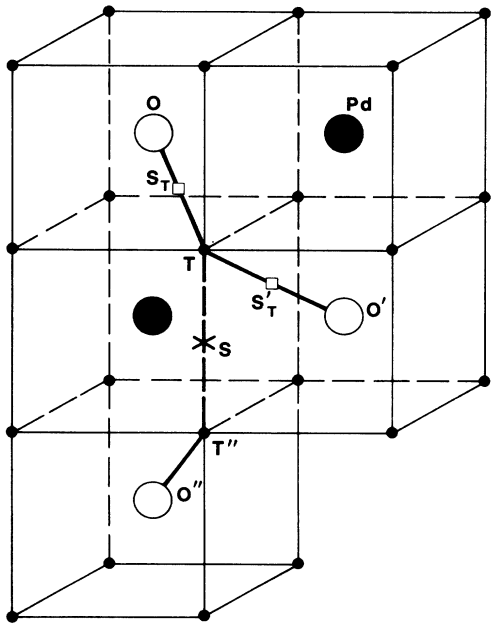

FIG. 7. The structure of fcc Pd. Small circles are tetrahedral sites, large solid circles, Pd; large open circles are octahedral sites favored by H. Paths shown by heavy solid and dashed lines are described in text.

hedral site, a jump was recorded and the assigned octahedral site changed. There are nuances in the criteria for response to the changes which are discussed in Appendix A, but these nuances do not affect 95% of the jumps which fall easily into a pattern in which two coordinates change by $\pm a/2$ and one does not change. This is strong justification for our subsequent modeling and analysis based on NN hopping. The remaining less than 5% of the jumps may nonetheless be of some interest for further theoretical, simulation, or high-resolution experimental studies, so their analysis is treated in Appendix A. That Appendix should also be useful to a reader interested in the problem of how jumping processes can efficiently be extracted from an overabundance of trajectory data.

The small fraction of non-NN jumps cannot explain the q dependence of Γ_q and in fact can be ignored within the statistical precision of ours or Gillan's simulation results for experimental quantities such as Γ_q. The key to non-CE instead lies in the distribution of the time between jumps, the residence time. Figure 8 displays the distribution of residence times obtained from the jump analysis. For the CE model the distribution of times would be a single exponential. The curve shown deviates from this in two obvious ways. First, there is a finite rise time (about one vibration period of hydrogen) which reflects the finite time to traverse the distance between two sites. The second effect is a decidedly nonexponential decay. The plot of the logarithm of the distribution function shown in Fig. 9 indicates that a reasonable fit can be obtained with two exponentials, with time constants of 0.13 and 1.00 ps at 975 K and of 0.18 and 4.00 ps at 700 K. The fast time constant is approximately the same at both temperatures whereas the long-time constant decreases by a factor almost as large as the decrease in the diffusion coefficient. The solid lines in Fig. 9 are

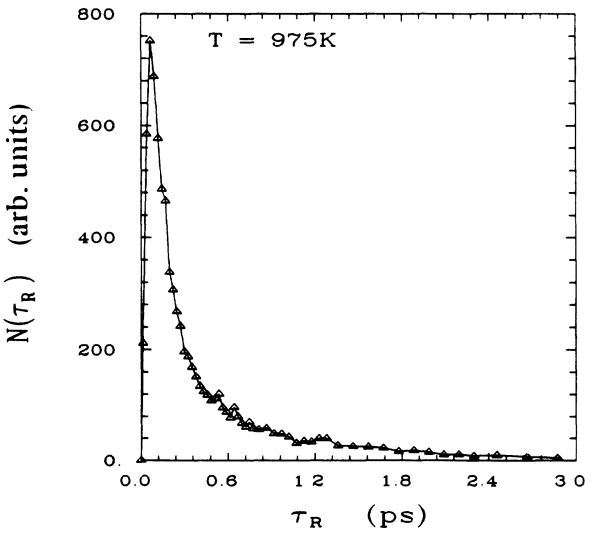

FIG. 8. The distribution of residence times for 975 K. The data have been analyzed with a variable bin width, represented by the time spacing between points. The points have been connected by lines to guide the eye. The nonexponential character of the decay and the finite rise time are evident.

fits with the two-step model discussed in the next section.

The above nonexponential distributions will produce a much stronger impression of "burst of jumps" than a CE distribution, but the jumps do not appear to be correlated. A measure of correlation between successive jumps is given by the function

$$C_\nu=(\langle\tau\tau_\nu\rangle-\langle\tau\rangle\langle\tau_\nu\rangle)/(\langle\tau^2\rangle-\langle\tau\rangle^2)\ . \tag{5}$$

Here τ is the residence time after a given particle makes an arbitrarily selected jump and τ_ν is the residence time for the same particle after it has made ν further jumps, i.e., $\nu=1$ corresponds to the very next jump. If the joint probability of successive jumps $P_\nu(\tau,\tau_\nu)$ is the same as the product of the independent probabilities $P(\tau)P(\tau_\nu)$, the jumps are uncorrelated and $C_\nu=0$ for $\nu>0$. We find from our simulations that $|C_1|<0.01$. Thus the difference from the CE model is in the jump distribution function and correlations are negligible.

The concept of independent jumps is reinforced by the distribution of the cosines of the angles between successive jumps. The average of this quantity for all jumps in the 975-K sample was -0.009 ± 0.004 indicating very little correlation. However, it does appear that the jumps separated by times less than one hydrogen vibration period have a significant positive value for the average, and this appears to be compensated by a negative average for the jumps which follow in the next hydrogen vibration period. Thus the lack of randomness in direction is lost in a very short time, and will not affect the QNS linewidth which reflects the behavior over longer times.

The two-exponential fits suggest that jumping is a two-step process. It is physically plausible to postulate that the first and slow step is the activation of a hydrogen atom from typical thermal energy to values which allow jumping over the barrier. The second and rapid step corresponds to the energetic atom finding an energetically allowed path to adjacent sites. It is recognized that the barriers to jumping are not static and the motion of the Pd atoms play a role in the "finding" of a path as well as in the transfer of energy to and from the hydrogen. The mathematics of a model with these features is developed in the next section. We also argue there that the degree of non-CE behavior is strongly affected by how soft the Pd-H potential is at short distances and we present further simulation data in support of this.

III. SIMPLE HOPPING MODEL

The two processes, energy transfer to the lattice and hopping while in the excited state, can be described schematically by sorting the classical continuum of states into two groups. One group comprises all states of typical thermal energy and localized about an equilibrium site. The states in this group which are localized at a given site will be referred to as the group states of a single hydrogen atom at that site. The second group includes all states which have sufficient energy to hop between sites. We consider these states also to be localized at an equilibrium site, but to have a transition rate W to other states of this group localized on neighboring sites. Members of the second group localized at a particular

site will be referred to as the excited states of an individual hydrogen atom at that site. In this model, the process of energy transfers between the hydrogen and the lattice are described by the transition rates w' from the ground state to the excited state and w for the reverse process. Detailed balance requires that $w'/w=(N/N')e^{-\Delta/k_BT}$ where N and N' are respective numbers of states in the excited and ground groups, and Δ is the effective energy difference for the two groups. Δ is nearly the same as the activation energy for diffusion. The ratio N/N' can be quite large for $k_BT \ll \Delta$ since $N \approx k_BT\rho(\Delta)$ and $N' \approx k_BT\rho(k_BT)$ where $\rho(E)$ is the density states, which increases rapidly with E owing to much less localization at the saddle point. A similar two-step model has been proposed as a possible explanation for non-CE behavior seen in $NbH_{0.02}$ at high temperature.[5] As noted in the discussion following Eq. (10), there is physical similarity between this model and that of hopping between traps[9] which has been used to explain scattering data in impure systems. Indeed a one-to-one correspondence exists between parameters of the two models, as shown below. We also note that the deep level of the well could be a self-trapping state induced by lattice distortions instead of the static level pictured here, without altering the basic equations.

The two-level picture is an extreme simplification of the classical simulation model in which there is a continuum of states. It nonetheless can provide physical insight and reproduces features of the simulation remarkably well. We regard this as evidence that, even in the classical model, the concept of excitation to "hopping states" is useful. One obvious shortcoming, however, is that the model uses time-independent transition probabilities in equations given below. Such probabilities can be valid only for times long compared to vibrational periods or transit times and thus preclude description of the finite time required and seen in the simulations before any jump can occur.

The rate equations for the model are

$$dm_i/dt=-(W+w)m_i+w'n_i+(W/Z)\sum_j m_j \ , \quad (6)$$

$$dn_i/dt=-w'n_i+wm_i \ . \quad (7)$$

Here n_i and m_i are, respectively, probabilities of finding a particle at site i in the ground and any one of the excited states and the summation is over the Z sites j which are neighbors of i. The equations are readily solved in terms of the wave-vector components $m_q=\sum_j m_j e^{i\mathbf{q}\cdot\mathbf{r}_j}$, with a similar definition for n_q and the sum going over all sites $\mathbf{r}_j$. Both m_q and n_q have a two-exponential decay characterized by a fast rate Γ_q^+ and slow rate Γ_q^- given by

$$\Gamma_q^{\pm}=\tfrac{1}{2}[w+w'+W(1-\gamma_q)]\pm\tfrac{1}{2}\{[w+w'+W(1-\gamma_q)]^2-4w'W(1-\gamma_q)\}^{1/2} \ , \quad (8)$$

where γ_q is the same as in Eq. (1). The relative amplitudes of the fast and slow components in the decay of $m_q(t)$ and $n_q(t)$ depend on the initial conditions. An initial Boltzmann distribution corresponds to $wm_q(0)=w'n_q(0)$. Since the probability that a particle is at site i at time t is given by $p_i(t)=m_i(t)+n_i(t)$, it follows that the decay of a thermal equilibrium density fluctuation $S_q(t)=\langle p_q(t)p_{-q}(0)\rangle/\langle p_q(0)p_{-q}(0)\rangle$, where the triangular brackets indicate thermal average, is given by

$$S_q(t)=\varepsilon_q e^{-\Gamma_q^+ t}+(1-\varepsilon_q)e^{-\Gamma_q^- t} \ . \quad (9)$$

For the Boltzmann initial conditions given above and corresponding to thermal equilibrium, we have $\varepsilon_q=[W(1-\gamma_q)w'/(w+w')-\Gamma_q^-]/(\Gamma_q^+-\Gamma_q^-)$. If $w'/w \ll 1$, corresponding to low temperature, or for $q\to 0$ it is easy to see that $\varepsilon_q \ll 1$ so that the decay is nearly single exponential at the slow rate Γ_q^-. It in fact turns out that $\varepsilon_q \sim < 0.1$ for all of the cases where we have fit the model to data, even for large q and w'/w comparable to unity. It is also valid to expand the square root in Eq. (8) for almost all cases of interest, so an adequate approximation is to take the decay rate

$$\Gamma_q=\Gamma_q^- \approx \Omega(1-\gamma_q)/[1+f(1-\gamma_q)] \ , \quad (10)$$

where $\Omega=w'W/(w'+w)$ and $f=W/(w+w')$. Equation (10) reduces to the CE Eq. (1) for $f \ll 1$, but shows strong departure from CE for large q ($1-\gamma_q$ not small) if $f \gtrsim 1$, as illustrated in Fig. 4. The coefficient of f is negligible for $q\to 0$, and there is diffusion with a coefficient $D=(\delta^2/6)\ w'W/(w'+w)$ [see discussion under Eq. (1) for relation between D and Ω].

The above solutions are formally equivalent to those for hopping in the presence of traps.[9] Here the ground states play the role of traps, $w/(w+W)$ is the probability of getting trapped before hopping to another site, and w' is the rate to escape from a trap. If one makes the replacements $w'=1/\tau_0$, $w=1/\tau_1$, and $W(1-\gamma_q)=\Lambda(Q)$, the decay rates in Eq. (8) are seen to be the same as in Eq. (20) of Ref. 8, and the expression for ε_q given under Eq. (8) is identical to R_1 given in Eq. (21) of Ref. 8.

The distribution of residence times is obtained from the solution of Eqs. (6) and (7) with the final term on the right-hand side of Eq. (6) set to zero, since it represents returns to the initial site which are not considered in calculation of the probability for making a single jump. The initial conditions are $m(0)=1$ and $n(0)=0$, since $t=0$ now is the time a particle arrives at a site, in which case it must be in an excited state. The quantity $p(t)=m(t)+n(t)$ represents the probability that the particle has not jumped up to time t, so $-(dp/dt)\delta t$ is the probability that the particle jumps between time t and $t+\delta t$, and we therefore take $P_r=-dp/dt$ to represent the distribution of residence times, whereby

$$P_r=A_re^{-\lambda^+ t}+B_re^{-\lambda^- t} \ , \quad (11)$$

where $\lambda^{\pm}=\frac{1}{2}(w+w'+W)\pm\frac{1}{2}[(w+w'+W)^2-4w'W]^{1/2}$ are the same as the rates derived from Eq. (7) with $\gamma_q=0$. The coefficients are in the ratio $A_r/B_r=(\lambda^+-w')/(w'-\lambda^-)$. In contrast to the situation for $S_q(t)$, the coefficient of the fast exponential can be appreciable at all temperatures. This is because the distribution is given by dp/dt, which enhances importance of the fast exponen-

tial. In the $w'/w \ll 1$ limit, $A_r/B_r=(1+f)^2 w/w'$. The mean residence time is given by $\tau_r=(A_r/\lambda^{+2}+B_r/\lambda^{-2})/(A_r/\lambda^{+}+B_r/\lambda^{-})$, which may be shown to give $\tau_r=(w'+w)/w'W$. By comparison with the expression under Eq. (10) we see that $\tau_r=1/\Omega$ so that, as expected, the diffusion coefficient is proportional to the inverse of the mean residence time.

As shown in Figs. 4 and 9, the model gives a reasonable fit to Γ_q and the time distributions in spite of its simplicity. The complete expression in Eq. (8) was used for Γ_q^- rather than the approximation of the second equality in Eq. (10) for the fitting routine and in the figures. The distribution was fit only for times greater than the time t_p at which it peaks, since the transit time effect is not included in the model. The fitting constants were constrained so that the total number of jumps (and thus the average residence time) is given correctly by assigning the jumps before t_p to a single bin centered at $t_p/2$. The fitted exponentials and amplitudes were consistent with the following values for parameters of the model: At 975 K, $W=3.7\pm0.4$ ps^{-1}, $w=2.4\pm0.5$ ps^{-1}, and $w'=1.9\pm0.1$ ps^{-1}. At 700 K, $W=2.1\pm0.5$ ps^{-1}, $w=2.5\pm0.5$ ps^{-1}, and $w'=0.61\pm0.05$ ps^{-1}. The ratio of A_r/B_r calculated from these data agree well with that from the jump distribution if the time t_p is considered the zero of time for the exponential distribution, as if there were a constant delay. (The deconvolution of a distribution of transit times would be more realistic.) The fits in Fig. 9 are meaningful only for points after the peak.

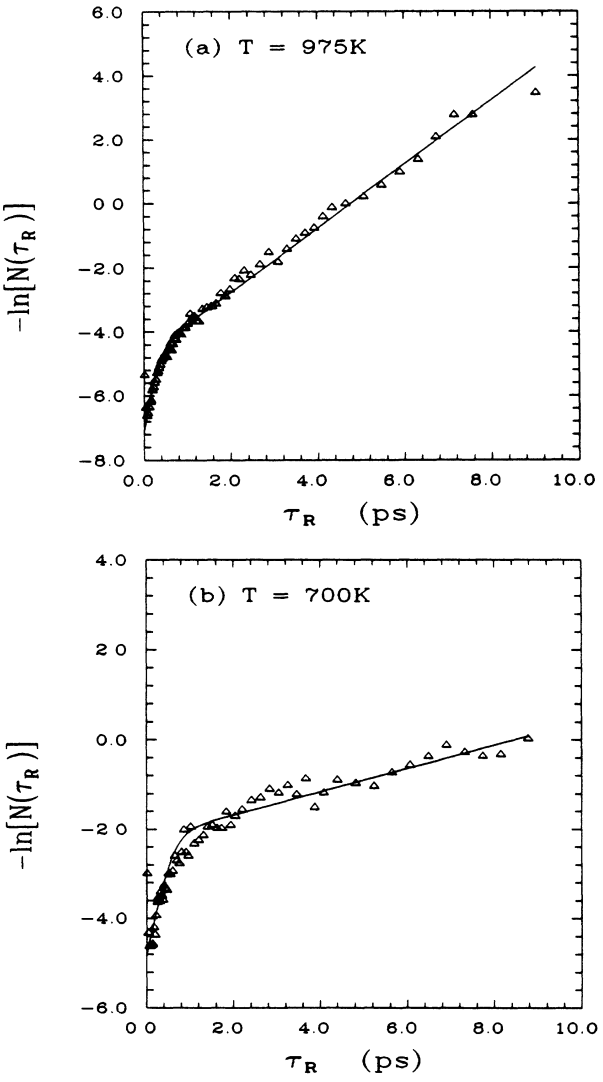

FIG. 9. Semilogarithmic plots of the residence time distributions. The solid curve is the sum of two exponentials with parameters obtained by a coordinated fitting of the distribution function and Γ_q data with the two-step model as described in the text: (a) 975 K and (b) 700 K.

The above rate parameters give small values of ε_q (less than 0.13 in all cases). The effect of nonzero ε_q for long times is to change the intercept in the semilog plot of Eq. (3) from $\langle u^2\rangle q^2$ to $\langle u^2\rangle q^2-\ln(1-\varepsilon_q)$. Our fits give values for $\langle u^2\rangle$ not significantly different from experiment, and the correction due to ε_q is less than the combined errors of the experiments and our simulation data.

The large uncertainty in W and w is due to the strong correlation in the effects of these two parameters. The fit requires w' and w to be comparable even though the Boltzmann factor $e^{-\Delta/k_BT} \ll 1$ at the temperatures considered. This is explained by a large value for N/N' as was anticipated. The temperature variation of the ratio w'/w yields a $\Delta\approx0.24$ eV, somewhat lower than the 0.29 eV activation energy for diffusion determined from the simulation. The diffusion coefficient in this model, as noted above, is proportional to $w'W/(w+w')$ which does have a temperature variation consistent with 0.29 eV. The temperature dependence of W corresponds to an activation energy of 0.12 eV. A more realistic model would have a group of levels, so the activation energies of w' and W in the overly simplified two-level system represent averages which should not be taken too literally in view of the crudity of the model, which was designed primarily to give a simple physical picture.

The crucial parameter in determining the departure of Γ_q from CE is $f=W/(w+w')$. Our simulations (Fig. 10) show that a harder-core metal-hydrogen potential gives much better agreement with CE than the relatively soft one used by Gillan and in our first studies. This implies that, within the context of the model, the stronger repulsion at short distance leads to a reduction of f which may be understood as follows. The hopping process requires trajectories which enter a narrow channel between larger site volumes in which the particle resides most of the time. For hopping between interstitial sites in the fcc lattice these "channels" are through the saddle point at the center of a triangle (face of tetrahedron) of close-packed metal ions. f is the ratio of the probability that an excited particle will pass through the channel to the probability that it will drop into the ground state by energy loss. Because of the much shorter metal-hydrogen distance at the saddle point than at the equilibrium octahedral site, the dominant effect of increasing the repulsion at short distances is effectively to shrink the cross section of the channel. This leads to a reduced probability for transitions out of the site and thus a reduced f.

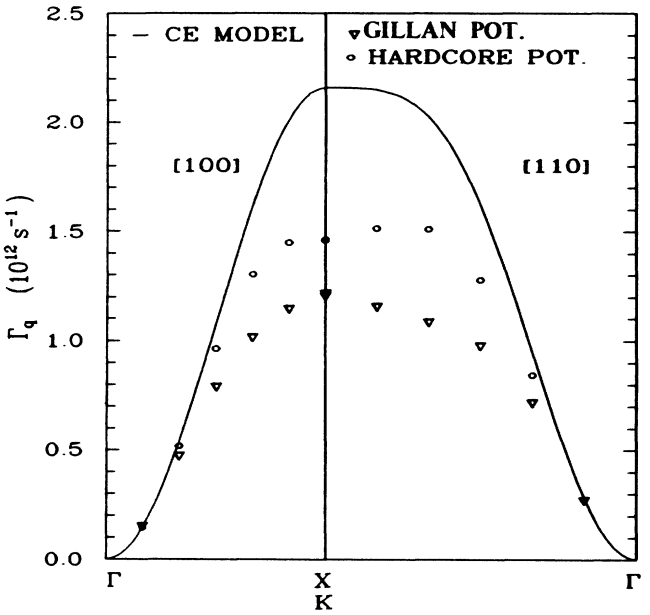

FIG. 10. The effect of a harder core on Γ_q. The CE result and the results for the Gillan potential are as in Fig. 1. The value of Ω for the harder-core potential was adjusted to agree with that of the Gillan potential at small q.

Figure 10 shows the effect of a harder core on the QNS linewidth. The harder core was implemented by changing the exponential relaxation length of $V_{\text{Pd-H}}$ by a factor of 15 for distances less than 1.65 Å while maintaining continuity of the potential and the force. The distance 1.65 Å is slightly smaller than the unrelaxed equilibrium Pd-H distance at the saddle point S_t. Thus the changes in potential do not affect the static barrier minimum nor the low amplitude vibrational frequency of the H. Within the context of the two-level model and the above discussion, the major effect should be to decrease W without changing w or w'. Thus, according to the results and definitions given in conjunction with Eq. (10), f and D should be decreased by the same amount. This is fairly well borne out. The data in Fig. 10 are consistent with f having decreased by a factor of 1.8 in going to the harder core, the value of D was found to have decreased by the factor 2.1 from analysis of $\langle r^2 \rangle$ versus t.

IV. SUMMARY AND DISCUSSION

We have done a molecular-dynamics (MD) simulation of hydrogen hopping in PdH_x with both the same potentials used by Gillan and a modified hydrogen-metal one with a harder core. We have further established criteria for identifying when jumps occur and defining residence times. For the same potentials, our results for the diffusion coefficient D and width Γ_q of the quasielastic neutron scattering (QNS) peak agree with Gillan, but we have a different interpretation. Gillan attributed the difference between Γ_q and the simple Chudley-Elliott (CE) result for nearest-neighbor hopping to a preponderance of non-nearest-neighbor jumps (or correlated nearest-neighbor jumps). Our statistical examination of the jumps, however, reveals mostly uncorrelated nearest-neighbor jumps, but the distribution of jump times is highly nonexponential. We believe this accounts for the non-CE behavior and have presented a simple two-level hopping model in support of this contention.

The harder-core potential changes the wave-vector dependence of Γ_q considerably, bringing it into much nearer agreement with CE. We presented a physical reason for this based on the reduction of density of states or classical paths for passage through the saddle point when there is added short-distance repulsion. This decreases the probability of jumping to a new site relative to the probability of a particle thermalizing at the site to which it has just jumped. The ratio of these probabilities, defined as f, is a crucial parameter of the two-level model. CE behavior requires $f \ll 1$.

Thus we conclude that disagreement between the MD simulations and QNS data which show a CE Γ_q for PdH_x does not necessarily reflect quantum or electronic effects but only a high sensitivity of the dynamics to the choice of potentials. It is not clear, however, whether all of the non-CE behavior is due to the relatively soft core, since we have not been able to achieve complete agreement with CE even by going to a very hard-core potential. There are two obvious possible difficulties which could make MD invalid even with the correct potentials and without the electronic effects which Gillan speculated might be important. The first is quantum effects, which can be much more severe with hydrogen in metals than, say, with fluorine in superionic conductors because of the large mass difference. The main quantum effect on hopping is tunneling. Tunneling of hydrogen in metals, at least from excited states, is well known to occur at low temperatures.[10] But it seems unlikely to be important in PdH_x at the highest temperature of the simulation, 975 K, which is larger than $\hbar\omega/k_B = 766$ K where ω is the hydrogen vibrational frequency in Pd. The observed Arrhenius behavior of D in this temperature range with a prefactor of the order of magnitude of the vibrational frequency also argues in favor of purely classical over-barrier hopping. A further point is that, in terms of our two-level model, tunneling might be expected to increase f and thus give even stronger departure from CE.

A second possible problem with MD is the small sample size. Our main argument against this is the observed size-independence of the results. We have also given some analytical consideration to the effect of the finite number of lattice phonon modes as described in Appendix B. The conclusion reached there is that the sample should have been large enough effectively to treat the number of modes as infinite. However even for an infinite lattice the light mass or equivalently high vibration frequency of hydrogen makes for relatively inefficient energy transfer between the metal lattice and hopping interstitial, which is at the heart of non-CE behavior.

We conclude that wave-vector dependence of QNS might be non-CE even in a regular lattice with nearest-neighbor jumps, which has already been suggested[5] in work on $NbH_{0.02}$. It is worthwhile to ask which lattice types favor non-CE and why PdH_x does seem to give CE. According to our physical arguments, CE behavior will

be observed if the density of states for a particle localized at an equilibrium site but in an excited state near the top of the well is large compared with the density of states at the saddle point. A simple measure of this could be the ratio $(r_e/r_s)^2$ where r_e and r_s are the respective hydrogen-metal distances (unrelaxed) at the equilibrium and saddle points: the larger r_e/r_s, the more likely CE to be obeyed. For fcc, assuming the saddle point to be at the center of the face of a tetrahedron as mentioned above, we have $(r_e/r_s)^2=1.49$, 1.12 for equilibrium octahedral (o) and tetrahedral (t) sites. For hopping between t sites in bcc, the ratio is $(r_e/r_s)^2=1.10$. On this basis, it may not be surprising that PdH_x, where the jumps are between o sites in fcc, gives agreement with CE. The small value for bcc is consistent with the above-mentioned data[5] in Nb. However, quantum effects are much more important in the bcc metals and may cloud the issue, so the most clear-cut test might be a QNS study of metals such as ThH_x or LaH_x where the α phase is fcc and the hydrogen is thought to reside at t sites. It also should be noted that although a QNS study of Γ_q may provide the most direct evidence, comparison between diffusion and NMR relaxation or internal friction could also be useful. This is because the latter two are most affected by single jump processes and thus tend to measure Γ_q near the zone boundary, whereas diffusion probes Γ_q for $q\rightarrow 0$.

A final comment is that, in the simplest view, the 20% concentration used in these simulations should have reduced the jump rate W in our model by 20% owing to blocking effects, but had no effect on w or w'. One would therefore expect that lower concentrations would lead to a larger f in the model and thus show even more deviation from the CE model. Preliminary results indicate this to be the case.

ACKNOWLEDGMENTS

This work was aided by a grant to one of the authors (JWC) by the Association of Western Universities, and by a sabbatical leave from the University of Kansas. John Noe gave valuable advice and information which accelerated the computation. We thank Brian Dodson for valuable practical advice on the molecular-dynamics techniques, and Sam Myers for encouragement, support, and valuable critiques. Work at Sandia National Laboratories supported by the U.S. Department of Energy under Contract No. DE-AC04-76DP00789.

APPENDIX A: APPROXIMATION OF THE DIFFUSION MOTION BY DISCRETE JUMPS

We describe here in detail the criteria that we have investigated for determining the occurrence of a jump. As described in Sec. II the hydrogen atoms are initially assigned to octahedral sites nearest their true positions. Subsequently the averaged displacements from the last assigned site rounded to multiples of $a/2$ are examined. These displacements include metal-ion sites as well as the octahedral sites at which hydrogen normally resides. The first six of these are shown in Fig. 11 and enumerated as $a-f$. More distant ones are grouped into a class g. Our program responds to these signals so to track the position of the hydrogen by assigning NN and NNN jumps in a manner as follows. Class-a displacements would indicate a move into a Pd site and must be either noise from large excursions or, as is more likely, a jump in progress. We ignore these since if it is a jump in progress, it will evolve to a higher class. Events belonging to the remaining classes are regarded as jump events, so the assigned octahedral site is changed. As seen in Fig. 11, the new site cannot be assigned unambiguously for classes c and e, and this can lead to problems in subsequent tracking of the particle's motion and thereby assignment of displacements into the proper classes.

For events of class b the response is obvious. This is the signature of a NN jump between octahedral sites. When this event occurs a single jump is recorded and the hydrogen is assigned to the indicated nearest-neighbor site. For each of the jumps called by the program, the time since the last jump and the cosine of the angle between the current jump vector and the last jump vector are recorded.

Events of class c probably represent a NN jump and a second jump that is in progress. The program arbitrarily treated such events as a NN jump corresponding to the x and y coordinates, thus reducing the residual to a class a.

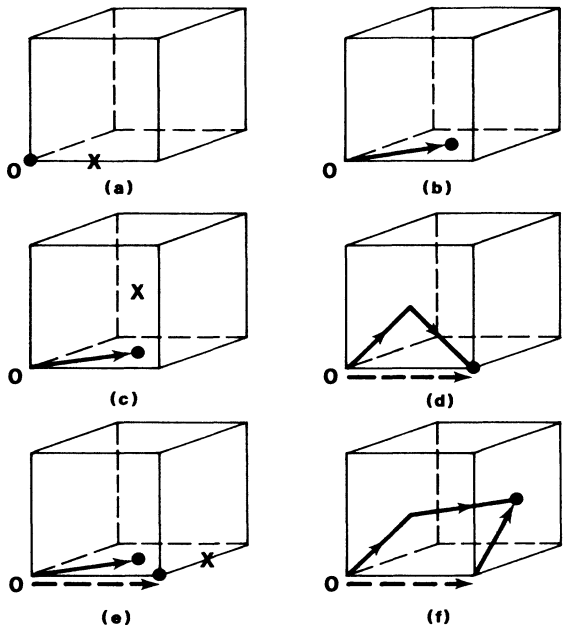

FIG. 11. Closest six displacements in units of $a/2$ into which position changes are grouped. Initial position is indicated by 0. In a, c, and e the final position is at a metal atom site denoted by $\times$. In these cases possible (but not necessarily unique) locations of the octahedral site to which particle is assigned are shown as solid circles. Solid lines with arrows indicate NN jumps, while dashed lines are NNN jumps. Different possible combinations of NN and NNN jumps to reach the same final site are shown for d and f.

We could equally well have assigned the new site to one of the two for which the z coordinate changes, so this presents an ambiguity as noted above.

Class-d events could either be direct NNN jumps via the $0 \rightarrow S_t \rightarrow T \rightarrow S \rightarrow T'' \rightarrow S_t'' \rightarrow 0''$ path which avoids nearest-neighbor octahedral sites, or be two unresolved NN jumps, as indicated in Fig. 11. Having identified and followed several trajectories, we believe that most class-d events are of the former type, and therefore all class-d events are taken as NNN jumps except where noted otherwise.

Events of class e can be interpreted two ways: as a NNN jump and another jump in progress, or as a NN jump and another jump in progress. Likewise, events of class f can be interpreted as a NNN jump and an overlapping NN jump, or as two NN jumps. The events are so rare that the distinction is not important, but we have results for both interpretations.

For events of class g, our program records the unusual occurrence and assigns a NN jump which will reduce the residuals. The sparsity of these events (see Table I and accompanying discussion) did not warrant more sophisticated analysis. Also as seen in Table I, the total number of events not in classes a, b, or d, which lead to ambiguities, fortunately is quite small.

In all responses, errors can be made because of noise. If a class-b signal is noise, a spurious jump will be assigned and then its exact inverse applied on the next evaluation cycle. In all cases the presence of noise will tend to produce an excess of jumps and bias the average of the cosine of the angle between jumps toward negative values.

In addition to the nuances in the response to the rare events there is another fine-tuning effect that should be considered in relation to noise. Observations of the trajectories show that hydrogen atoms often make excursions to the tetrahedral sites which do not result in jumps to octahedral sites. For such excursions the coordinate changes are centered at $a/4$, and thus strict rounding to nearest integer multiples of $a/2$ will frequently produce a class-a event and with decreasing frequency class-b and -c events. Such noise is reduced if the rounding is biased so that a change of magnitude greater than $0.375a$ is required to produce a signal of $a/2$. We normally applied this bias, but for comparison one set of results are shown in Table I without the bias.

Table I shows $\langle \cos\theta \rangle$, the average of the cosine of the angle between successive NN jumps and the number of events obtained in each class in the analysis of 2×10^5 sets of averaged hydrogen coordinates, for five variations in the criteria and averaging times. Also shown in the table is the total number of NN and NNN neighbor jumps assigned. These are related to the number in the bins according to the responses to each class of events. The simulation temperature was 975 K.

The first row, identified as analysis I, used NNN neighbor jumps in the responses to classes d, e, and an NNN plus an NN for class f and used biased rounding of the coordinate changes. The results of analysis I are those used for Fig. 9 and in comparisons with the two-step model. The second row, analysis II, is the same as I except unbiased rounding was used. For both analyses the number of NN jumps is the sum of classes b, c, f, and g, and the number of NNN jumps is the sum of classes d, e, and f. The number of jumps in class b has changed by only 1% but there is a change in $\langle \cos\theta \rangle$ toward negative values for analysis II, indicating more jumps that were made and immediately reversed as expected from increased noise. Also the number of events in class a, the clear-cut noise indicator, is more than twice as large without the bias. The actual jump distribution and the approximation of the total motion by the NN jumps alone is not significantly affected by the bias. For both of these analyses the total number of NNN jumps assigned is less than 2% of all jumps and they have an insignificant effect on the calculation of Γ_q. However, the following analyses show that their inclusion in the jump analysis is absolutely necessary for smooth tracking of the motion.

In analyses III-V summarized in Table I, the rounding bias has been applied, but we have experimented with variations in the responses to the class d, e, and f signals. For III, class-d events were taken as NNN as before, but only NN jumps were used for e and f. A more careful analysis would then have assigned two NN jumps for class f, as suggested by Fig. 11, but we assigned only one NN jump to a site which minimized the residual. Thus the number of NN jumps is now the sum of classes b, c, e, f, and g while the number of NNN jumps is just the number in class d. The actual effect on the approximation by single NN jumps alone and on the jump distribution is again not significantly affected by this change, however the number of events in class a has increased

TABLE I. Results of jump analyses for five variations of jump criteria, responses, and averaging times. The variations are identified by Roman numerals in the first column and are defined in the text. The columns labeled NN and NNN are the number of NN and NNN jumps assigned, $\langle \cos\theta \rangle$ is average of the cosine of the angle between successive NN jumps, the columns labeled a–f are the number of events in the six classes defined in Fig. 11, and column g represents all events not belonging to a–f.

	NN	NNN	$\langle \cos\theta \rangle$	a	b	c	d	e	f	g
I	8996	154	−0.0086	4374	8943	3	104	9	41	0
II	9075	364	−0.0327	16131	8845	103	229	94	31	2
III	8864	121	−0.0007	13922	8566	141	121	120	37	0
IV	7643	0	+0.0408	81603	5963	982	76	1127	47	364
V	8183	415	+0.0026	6704	7820	127	179	147	89	17

dramatically which indicates inferior tracking of the motion.

In analysis IV only single NN jumps are allowed, whereby classes *e* and *f* are treated as in III but a class *d* event is simply ignored as if it were perhaps a NN jump in progress plus noise. The effect is dramatic as far as the distribution among classes is concerned, but the change in the number of NN jumps assigned which is now the sum of all classes beyond class *a* is not especially large. The value of $\langle \cos\theta \rangle$ for these jumps has increased considerably, because the tracking has been implemented with fewer jumps so that they must show an increased forward bias. Comparison of the diffusion constant calculated with these NN jumps with that from the mean-square distance versus time shows that there must also be some forward correlation in this case that extends beyond that of the successive jumps which is all that is indicated by $\langle \cos\theta \rangle$. The highly inferior tracking is shown by the over 80 000 class-*a* events. Perhaps surprisingly, the residence time distribution for the NN jumps obtained in analysis IV is not seriously altered from that shown in Fig. 9.

For analysis V, the bias, and responses were the same as for I, but the averaging time was made twice as long ($20t_s$). The changes *vis-à-vis* I are entirely predictable. The main effect is that the number of NNN jumps has increased from 154 to 415 and the number of NN jumps has decreased by about 800. This effect has arisen almost entirely by the fact that jumps which in analysis I were recorded as NN jumps with separations of $10t_s$ will now often be fused to give class-*d*, -*e*, and -*f* signals. Also the value of $\langle \cos\theta \rangle$ has increased somewhat as would be expected from the elimination of some pairs of canceling jumps. The distribution of residence times for the NN jumps is not significantly affected at times greater than $40t_s$. Of course the minimum residence time is now $20t_s$ and the peak is shifted from $30t_s$ to $40t_s$. Neither these changes nor the 5% of NNN jumps have an important impact on the calculation of Γ_q. It should be noted that the effect of these additional NNN jumps is largely replicated in analysis I by the extra NN jumps with short residence times. The additional 3% of so-called NNN jumps produced by analysis V represent trajectories which have actually passed rather close to an intermediate octahedral site (such as the path singled out by an arrow in Fig. 5), and the description as two NN jumps with a small time separation is a more accurate representation of the actual trajectory. In the comparison with the two-step model we have used the results of analysis I which includes 98% of all jumps as NN, and ignored the few NNN jumps. The small number of events outside of class *b* did not warrant more sophisticated treatment than discussed above, at least in this first largely exploratory effort. More precise analysis techniques could be developed along the lines we have used should the necessity arise to consider beyond-NN hopping in detail.

As pointed out in Sec. III, the model does not accurately represent the finite rise time of the residence time distribution, and for comparison with available QNS data the details of the initial parts of the distribution function are unimportant so long as the distribution after several H vibration periods is accurately predicted.

APPENDIX B: ENERGY TRANSFER FROM DISCRETE PHONON MODES

The hopping process requires the hydrogen to acquire sufficient energy from the vibrating metal lattice. If the frequency spacing between lattice modes is large, it might not be possible to establish the resonance conditions needed for effective interaction. Since the spacing is of the order of ω_D/N where ω_D is the debye frequency and N the number of metal atoms, small sample size can be important. To examine this question we have studied solution to the equation

$$d^2x/dt^2+\omega_0^2 x = F(t) , \tag{B1}$$

where $F(t)=(1/N)\sum_{k=1}^{N} A_k \cos(\omega_k t+\phi_k)$ in which the phases ϕ_k are random. This can describe the initial acquisition of energy from the lattice modes when the hydrogen position x is sufficiently near to equilibrium that it can be described by a harmonic oscillator of frequency ω_0. For simplicity we took a one-dimensional spectrum $\omega_k=\omega_M \sin(\pi k/2N)$, A_k independent of k and considered various values of N and ω_0/ω_M. The probability $Q(x,t)$ of the particle being at x at time t can be shown to be Gaussian in the limit $N\to\infty$. Our computations of $Q(x,t)$ at various x,t show that for $N=100$, roughly corresponding to the simulation if only longitudinal modes are considered, there is better than 1% agreement with the exact $N\to\infty$ expression, and even for N as small as 10 there are no major deviations. Hence we conclude, consistent with the size independence of the MD results, that discreteness of the finite-sample lattice modes should not be a problem.

[1]See, for example, J. J. Erpenbeck and W. W. Wood, Chap. 1, and J. Kushick and B. J. Berne, Chap. 2, in *Modern Theoretical Chemistry,* edited by B. J. Berne (Plenum, New York, 1977), Vol. 6.

[2]M. J. Gillan, J. Phys. C **19**, 6169 (1986).

[3]K. Skold, in *Hydrogen in Metals I,* Vol. 28 of *Topics in Applied Physics,* edited by G. Alefeld and J. Volkl (Springer, New York, 1978), Chap. 10.

[4]I. Anderson (private communication).

[5]V. Lottner, J. W. Haus, A. Heim, and K. W. Kehr, J. Phys. Chem. Solids **40**, 557 (1979).

[6]C. T. Chudley and R. J. Elliott, Proc. Phys. Soc. London **77**, 353 (1961).

[7]P. Schofield, Comput. Phys. Commun. **5**, 17 (1973).

[8]M. T. Hutchings, K. Clausen, M. H. Dickens, W. Hayes, J. K. Kjems, P. G. Schnabel, and C. Smith, J. Phys. C **17**, 3903 (1984).

[9]D. J. Richter and T. Springer, Phys. Rev. B **18**, 126 (1978).

[10]I. Svare, Physica B + C **141B**, 271 (1986).